ACS APPLIED MATERIALS & INTERFACES

Research Article

www.acsami.org

Rapid and Efficient Multiple Healing of Flexible Conductive Films by Near-Infrared Light Irradiation

Yang Li, Shanshan Chen, Mengchun Wu, and Junqi Sun*

State Key Laboratory of Supramolecular Structure and Materials, College of Chemistry, Jilin University, Changchun 130012, People's Republic of China

Supporting Information

ABSTRACT: Healable, electrically conductive films are essential for the fabrication of reliable electronic devices to reduce their replacement and maintenance costs. Here we report the fabrication of near-infrared (NIR) light-enabled healable, highly electrically conductive films by depositing silver nanowires (AgNWs) on polycaprolactone (PCL)/poly(vinyl alcohol) (PVA) composite films. The bilayer film has sheet resistance as low as 0.25 $\Omega \cdot sq^{-1}$ and shows good flexibility to repeated bending/unbending treatments. Multiple healing of electrical conductivity lose caused by cuts of several tens of micrometers wide on the bilayer film can be conveniently achieved by irradiating the film with mild NIR light. The AgNW layer functions not only as an electrical conductor but also as a NIR light-induced heater to initiate the healing of PCL/PVA film, which then imparts its healability to the conductive AgNW layer.

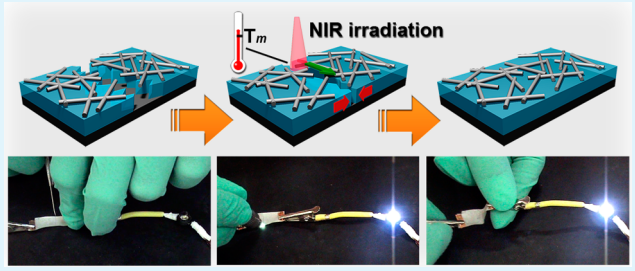

KEYWORDS: *conducting materials, light-response, materials science, polymer, self-healing*

INTRODUCTION

Electrically conductive materials and films are indispensable in the development of various electronic devices. An aging or mechanically damaged electrical connector or electronic component can ruin the circuit board and paralyze the entire electronic device. Nowadays, replacing a damaged circuit board with a new one is very uneconomical, considering the high integration density of circuit boards. Such a problem can be resolved by using electrically conductive materials that are capable of healing from damage to build electronic devices.[1,2] The concept of self-healing revolutionized the way scientists design artificial materials.[2−9] Self-healing materials can restore their mechanical properties or function after incurring damage. Inspired by examples in nature, various self-healing materials have been artificially developed in which healing is achieved through the release of a healing agent contained in the materials[10−15] or through the inherent reversibility of dynamic covalent bonds and noncovalent bonds.[16−27] Such materials can heal themselves in either an autonomic or nonautonomic way, depending on whether human intervention is required during the healing process.[18,19,28,29] Nonautonomic self-healing materials that require external assistance such as light, heat, humidity, and so forth to accomplish healing of damage are also regarded as healable materials. The use of conductive self-healing materials in developing electronic devices not only reduces the replacement and maintenance costs but also improves the reliability of devices.[1,2] Therefore, the fabrication of self-healing, electrically conductive materials has been the subject of extensive research.

Among the methods that have been developed for the fabrication of self-healing conductive materials, the capsule-based method, which utilizes polymeric microcapsules incorporated with electrically conductive species as healing agents, has been widely investigated.[30−32] The rupture of the microcapsules releases the encapsulated liquid conductive species, which then flows to the damaged area and restores electrical conductivity. Apart from eutectic Ga−In liquid metal alloy,[30] solid conductive species have to be coencapsulated into microcapsules with solvent to achieve flowability, thereby making the encapsulation process complicated and the capsules vulnerable to damage. Despite its autonomous self-healing nature, however, multiple healing in the same spot is impossible because of the depletion of conductive healing agents after a single damage. As an alternative to the capsule-based method, we developed a facile method to fabricate self-healing, electrically conductive films by depositing silver nanowires (AgNWs) on top of self-healing polyelectrolyte multilayer (PEM) films.[33] In this manner, the water-enabled self-healing ability of the PEM films is imparted to the electrically conductive AgNW layer. The method of imparting the self-healing ability of polymers to inorganic conductive materials has been successfully applied in the fabrication of self-healing electronic skins,[34] stretchable wires,[35] supercapacitors,[36] and heat-induced, self-healing semitransparent conductors[37] with multiple healing capabilities in a particular damaged spot.

Received: July 23, 2014
Accepted: September 2, 2014
Published: September 2, 2014

Therefore, this method is generally applicable in designing various self-healing conductive materials. The above-mentioned conductive materials achieve healing either by manually bringing the broken conductors into contact[34−36] or with the aid of water and heat.[33,37] For example, Pei and co-workers[37] fabricated heat-induced, self-healing conductive films composed of a healable Diels−Alder-based polymer film inlaid with an AgNW layer on its surface. This conductive film is healed at a temperature under 110 °C, which may exceed the tolerance of several plastic-based flexible devices. How to fabricate a highly conductive film that can be conveniently healed by an easily available method for multiple times is still a challenge. As for the stimulus that initiates the healing process, near-infrared (NIR) light demonstrates several advantages over water and heat, such as its mild quality and capacity to be delivered remotely and instantly with high accuracy to the damaged area. In this work, we report the fabrication of NIR light-enabled healable, highly electrically conductive, flexible films by depositing AgNWs on top of polycaprolactone (PCL)/poly(vinyl alcohol) (PVA) composite films. The resultant bilayer film shows good flexibility to repeated bending/unbending treatments. In addition, the produced bilayer film is highly conductive, with sheet resistance (R_s) as low as 0.25 $\Omega \cdot sq^{-1}$. Under mild NIR light irradiation, the conductive films can achieve multiple structural and electrical healing in the same damaged area without apparent loss in conductivity.

EXPERIMENTAL SECTION

Materials. PCL ($M_n \approx 80\,000$ g·mol^{-1}), PVA (87−89% hydrolyzed, $M_w \approx 85\,000$−$124\,000$ g·mol^{-1}), and polystyrene (PS) ($M_w \approx 200\,000$ g·mol^{-1}) were purchased from Sigma−Aldrich. All chemicals were used without further purification. AgNWs were synthesized according to a method described in literature.[38] The as-prepared AgNWs were centrifuged and redispersed in an ethanol solution to attain a concentration of 3.3 mg·mL^{-1}.

Fabrication of PCL/PVA Films. Silicon and poly(ethylene terephthalate) (PET) substrates were cleaned with O_2 plasma at 0.3 mbar under a power of 80 W for 3 min. The PCL/PVA films were fabricated by alternately spin-coating PCL and PVA on newly cleaned silicon or PET substrates. First, PCL dichloromethane solution (100 mg·mL^{-1}) was spun at 500 rpm for 5 s, followed by 1000 rpm for 1 min, to form a PCL layer on the substrate. Subsequently, PVA aqueous solution (10 mg·mL^{-1}) was spun at 500 rpm for 5 s, followed by 2000 rpm for 1 min, to form a PVA layer on the PCL layer. These two steps were repeated until the desired number of deposition cycles was achieved.

Instruments and Characterization. SEM images were recorded on a field-emission scanning electron miscroscope (XL30 ESEM FEG SEM). Film thickness was determined on a Veeco Dektak 150 surface profiler using a 5 μm stylus tip with 3 mg stylus force. As an alternative, film thicknesses were determined on the basis of their cross-sectional SEM images. Electrical resistance was measured via four-point-probe resistance measurements (RTS-8, Four Probe Tech, Guangzhou, China). A Keithley 2400 source meter was employed as a direct current (dc) source supply, as well as to record the currents passing through the circuit during healing of the AgNW/$(PCL/PVA)_6$ film by NIR light irradiation. Differential scanning calorimetry (DSC) measurements were performed on a Netzsch DSC-204 with a heating rate of 10 °C·min^{-1}. A thermocouple thermometer (TES 1310) with 0.5 mm K-type thermocouple sensor was employed to monitor the temperature of films. To measure the film temperature, the thermocouple sensor was pressed onto the film. The film around the thermocouple sensor was irradiated by NIR light and the temperature was recorded when the digital readout became stable. NIR light irradiation was performed at 812 nm with a laser diode source (HOTE NIR LOS-BLD system, Hi-Tech Optoelectronics, China). By use of the calibration curve provided by the manufacturer, the power density delivered to the sample was calculated as ~1 W·cm^{-2}.

RESULTS AND DISCUSSION

Fabrication of Thermally Healable PCL/PVA Films. The key step in this work is the fabrication of polymeric films that can heal themselves at low temperature. PCL, a thermoplastic with melting temperature (T_m) of around 60 °C, becomes moldable at temperatures above its T_m and returns to a solid state upon cooling. This low-temperature responsive property of PCL can be exploited in fabricating healable films. To achieve a precise film thickness, $(PCL/PVA)_n$ multilayer films (where n is the number of film deposition cycles) were fabricated by alternately spin-coating PCL dichloromethane solution (100 mg·mL^{-1}) and PVA aqueous solution (10 mg·mL^{-1}) on freshly cleaned silicon or poly(ethylene terephthalate) (PET) substrates. As shown in Figure 1a, the thickness

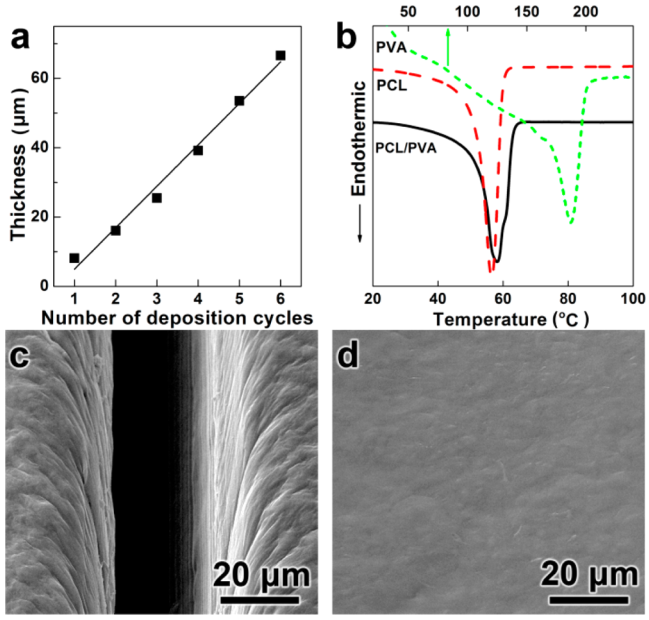

Figure 1. (a) Dependence of $(PCL/PVA)_n$ film thickness on number of deposition cycles. (b) DSC curves of PCL (red dashed line), PVA (green dotted line), and $(PCL/PVA)_6$ film (black solid line). (c, d) SEM images of $(PCL/PVA)_6$ film with a cut, (c) before and (d) after heat-induced healing.

of the PCL/PVA films increases almost linearly with the number of film deposition cycles. The linear deposition allows for convenient control of the film thickness by simply changing the number of film deposition cycles. A $(PCL/PVA)_6$ film has a thickness of ~67 μm, with the average thickness of each PCL and PVA layer being ~10.1 μm and ~30 nm, respectively. In the sequential spin-coating process, the ultrathin PVA layer can prevent dissolution of the previous PCL layer but cannot significantly alter the thermal-responsive property of the composite films. Hydrogen bonding between ketone groups of PCL and hydroxyl groups of PVA ensures firm adhesion between the PCL and PVA layers. In a control experiment, the successive spin-coating of PCL failed to produce a PCL film with a desirable thickness (Figure S1, Supporting Information). As proved later on, thick PCL film plays an important role in realizing healability. This explains why PCL/PVA composite film rather than neat PCL film is employed for the fabrication of healable conductive film.

Differential scanning calorimetry (DSC) measurements indicate that although PVA has a high T_m of ~187 °C, the PCL/PVA composite film has a T_m of ~58 °C, which is only 2 °C higher compared with pure PCL (Figure 1b). The slight increase of T_m in the PCL/PVA films is due to the relatively small amount of incorporated PVA. A cut roughly ~42 μm wide, which penetrated to the silicon surface, was made in the $(PCL/PVA)_6$ film with a scalpel (Figure 1c). The cut disappeared after the damaged $(PCL/PVA)_6$ film was heated on a hot plate at a temperature of 65 °C for 2 min, indicating that heating can enable healing of damage in the composite films (Figure 1d). Under increased temperatures, the $(PCL/PVA)_6$ film softens and becomes flowable, causing the fractured surfaces in the damaged area to come into contact and fuse together. In this way, the cut in the $(PCL/PVA)_6$ film is repaired. Despite the heat-enabled healing of the film, the cut in $(PCL/PVA)_6$ film cannot be healed by irradiating the damaged film with an 812 nm NIR light (~1 W·cm^{-2}). A thermocouple thermometer was used to measure the temperature of the NIR-irradiated area of the $(PCL/PVA)_6$ film, which was ~30 °C. This result is due to the inability of the PCL and PVA polymers to effectively absorb and transform NIR light into thermal energy (Figure S2, Supporting Information).

Fabrication of AgNW-Covered PCL/PVA Films. To exploit the NIR light-induced thermal effect to fabricate healable conductive films, an ethanol solution of poly(vinylpyrrolidone) (PVPON)-decorated AgNWs (3.3 mg·mL^{-1}) with diameter of ~100 nm and length ranging from 15 to 25 μm was drop-cast onto the $(PCL/PVA)_6$ film to produce a bilayer AgNW/$(PCL/PVA)_6$ film. As depicted in Figure 2a, the random orientation of AgNWs produces a meshlike AgNW film with a high density of wire−wire junctions, which is a key factor in the high conductivity of the AgNW film.[39−42] The as-prepared AgNW/$(PCL/PVA)_6$ film has R_s as low as ~0.25 Ω·sq^{-1}, which was measured via a four-point-probe resistance method. The conductive AgNW layer has a thickness of ~700 nm, as measured from the cross-sectional SEM image of the AgNW/$(PCL/PVA)_6$ film, which is shown in Figure 2b. Hydrogen-bonding interactions between hydroxyl groups of PVA and pyrrolidone groups of the PVPON-decorated AgNWs guarantee strong adhesion between the AgNW and $(PCL/PVA)_6$ layers. The AgNW/$(PCL/PVA)_6$ film deposited on the PET sheet is highly flexible and can endure repeated bending and unbending treatments.

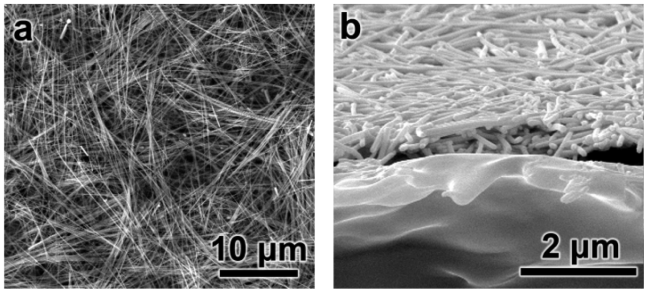

Figure 2. (a) Top view and (b) cross-sectional SEM images of an electrically conductive AgNW/$(PCL/PVA)_6$ film.

The currents passing through the AgNW/$(PCL/PVA)_6$ film remained almost constant during the entire bending process (Figure 3a). After the AgNW/$(PCL/PVA)_6$ film was bent to an angle of ~150° more than 1000 times, no reduction in film conductivity was observed (Figure 3b). Moreover, the AgNW layer and the AgNW/$(PCL/PVA)_6$ film did not separate or peel off from the PET substrate. The high flexibility and stability of the AgNW/$(PCL/PVA)_6$ films ensure the suitability of their application in fabricating flexible electronic devices.

NIR Light-Enabled Healing of AgNW/$(PCL/PVA)_6$ Films. The NIR light-induced healing of the AgNW/$(PCL/PVA)_6$ film was examined by connecting the film to a circuit with a light-emitting diode (LED) and a dc power supply. The voltage was set to 3.0 V (Figure 4a1). When the AgNW/$(PCL/PVA)_6$ film was cut across its entire width with a scalpel, the LED immediately went off (Figure 4a2). The cut resulted in a break in the electrical circuit as the current through the circuit became zero (Figure 4b). The cut, which was ~42 μm wide and penetrated to the underlying PET surface, broke the top AgNW layer as well as the bottom $(PCL/PVA)_6$ layer, signifying that the AgNW/$(PCL/PVA)_6$ film incurred severe damage (Figure 4c). Interestingly, the LED lit up again after the cut was exposed to 812 nm NIR light (~1 W·cm^{-2}) under ambient conditions at a temperature of 20 °C for 6 s (Figure 4a3). The LED became brighter with time, which indicated that the healing process continued under uninterrupted NIR light irradiation. The brightness of the LED became steady after 2 min of irradiation by NIR light. Repeated folding of the healed AgNW/$(PCL/PVA)_6$ film did not reduce the LED brightness (Figure 4a4), which shows that conductivity was completely healed through NIR light irradiation. A video recording of the

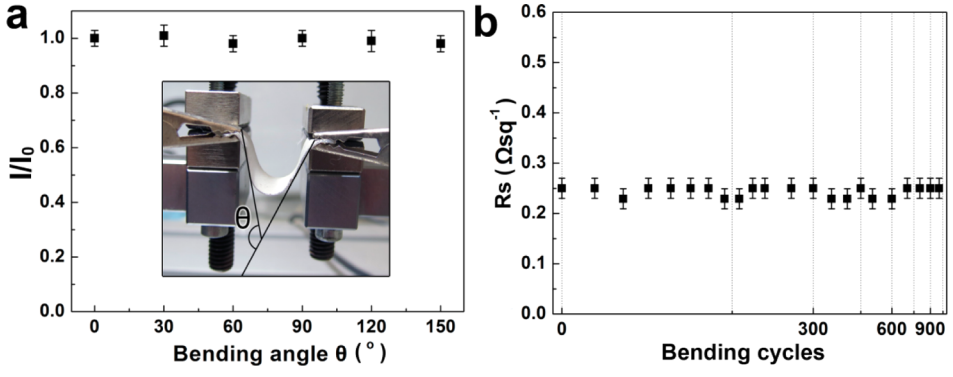

Figure 3. (a) Current changes in AgNW/$(PCL/PVA)_6$ film with applied voltage of 0.01 V as a function of bending angle (θ) from 0° to 150°. (Inset) Optical image of AgNW/$(PCL/PVA)_6$ film (3 × 1 cm^2) bent to 150°. (b) Plot of R_s of AgNW/$(PCL/PVA)_6$ film as a function of bending cycles. The film was bent to ~150° with a bending rate of 2 Hz.

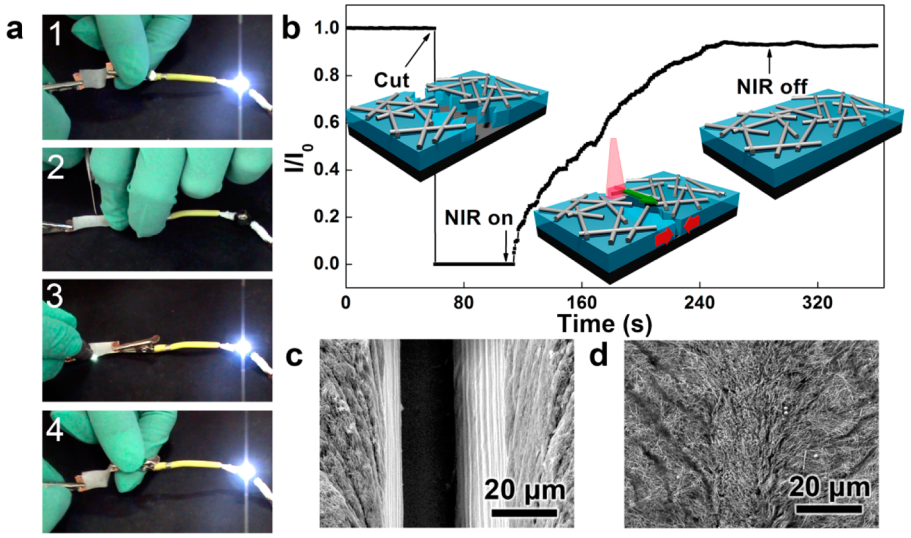

Figure 4. (a) Time profiles of healing of a cut on an AgNW/$(PCL/PVA)_6$ film connected to a circuit with an LED bulb: (1) as-prepared film; (2) the film is cut; (3) NIR irradiates on the cut to restore conductivity; (4) the healed film is repeatedly bent to demonstrate its high stability. The entire movie that shows the cutting/healing process is available in the Supporting Information. (b) Current changes in AgNW/$(PCL/PVA)_6$ film during a cutting/healing process. The cut was made at t = 60 s. NIR light irradiation was applied at t = 110 s and continued through t = 290 s. (c, d) SEM images of a AgNW/$(PCL/PVA)_6$ film with a cut, (c) before and (d) after being healed.

cutting and healing process can be found in the Supporting Information.

The healing of the cut AgNW/$(PCL/PVA)_6$ film was further characterized by recording the time-dependent currents passing through the circuit. As shown in Figure 4b, the current, which increased along with the duration of NIR light irradiation, was detected after 6 s of irradiation. The current reached a plateau, and up to ~94% of its original value was restored within 2.5 min of irradiation. Therefore, healing was accomplished within 2.5 min of NIR light irradiation. The SEM image of the healed AgNW/$(PCL/PVA)_6$ film provided in Figure 4d shows that the cut completely disappeared after NIR light irradiation. Under NIR light irradiation, the AgNWs, which absorb and convert NIR light into thermal energy,[43] function as nanosized heaters to raise the temperature of the bottom $(PCL/PVA)_6$ layer (Figure S2, Supporting Information). As measured by a thermocouple thermometer, the NIR irradiation was found to be capable of heating the damaged area up to ~65 °C. The $(PCL/PVA)_6$ film thus softens and flows to repair the cut in the same way as when the damaged film was directly heated. The strong interactions between the $(PCL/PVA)_6$ and AgNW layers allow for the simultaneous movement of separated AgNW layers toward each other. Finally, the separated AgNW layers reconnect, and electrical conductivity is thus restored. Although NIR light is less efficient in inducing heat generation of AgNWs compared with visible light, the temperature raised by NIR light is sufficiently high to induce healing of the $(PCL/PVA)_6$ film, owing to the low melting temperature of the polymer film. In a control experiment, AgNW/[polystyrene (PS)/PVA]$_6$ film was fabricated following the same procedure for fabricating AgNW/$(PCL/PVA)_6$ film. However, the AgNW/$(PS/PVA)_6$ film failed to heal a cut under the same NIR light irradiation (Figure S3, Supporting Information). Given the high temperature required to soften PS, healing a cut on a AgNW/$(PS/PVA)_6$ film was achieved by heating the film on a hot plate at a temperature of 130 °C for 10 min. Therefore, PCL is crucial in fabricating healable, highly electrically conductive films that allow for healing to be achieved by a low-power NIR light irradiation. It should be mentioned that although carbon nanotubes can convert NIR light into heat,[44] their conductivity is much lower than that of AgNWs.

A previous study shows that visible light irradiation can induce the welding of AgNW junctions whereas NIR light irradiation cannot, because visible light is more efficient than NIR light in inducing heat generation of AgNWs.[41] In the present study, the welding of AgNW junctions is deliberately avoided by using NIR light. The sliding or deformation of AgNWs can eliminate the stress produced during movement of the damaged AgNW layers. Compared with the physically jointed AgNWs, the welded AgNWs cannot slide or become deformed, which is unfavorable in terms of healing the damage in an AgNW/$(PCL/PVA)_6$ film. Moreover, the AgNW/$(PCL/PVA)_6$ film has a strong capacity to heal a damaged area multiple times. As shown in Figure 5a, after seven cycles of the cutting/healing process, in which the cuts were made within a width range of ≈0.5 mm on the film, R_s across the cutting–healing area increased only from 0.25 to 0.6 $\Omega \cdot sq^{-1}$. The SEM image in Figure 5b exhibits that the separated AgNW layer was closely connected after seven cycles of the cutting/healing

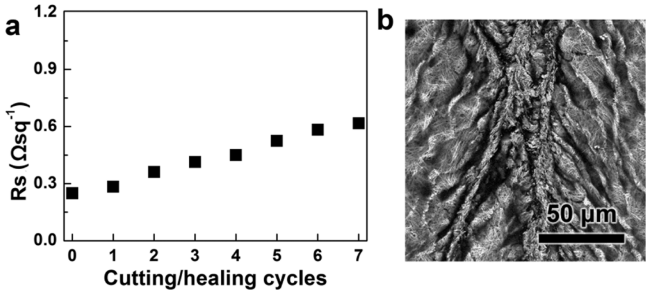

Figure 5. (a) Changes in sheet resistance of AgNW/$(PCL/PVA)_6$ film after multiple cutting/healing processes in the same region. (b) SEM image of the sample in panel a after seven cutting/healing cycles.

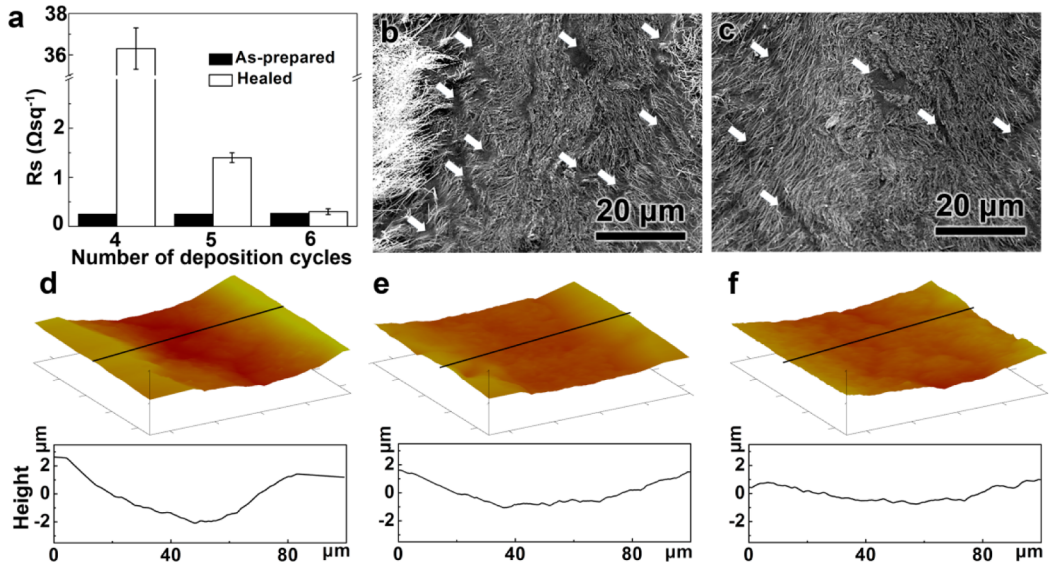

Figure 6. (a) Thickness-dependent changes in sheet resistance of the healed region in as-prepared and healed $(PCL/PVA)_n$ films, with n = 4, 5, and 6. (b, c) SEM images of (b) AgNW/$(PCL/PVA)_4$ film and (c) AgNW/$(PCL/PVA)_5$ film in the region after the cut was healed. Arrows indicate the gaps produced in the corresponding healed films. (d–f) AFM images and line scans of healable $(PCL/PVA)_n$ films with (d) n = 4, (e) n = 5, and (f) n = 6 in the region after the cut was healed.

process. The multiple healing of the AgNW/$(PCL/PVA)_6$ films considerably enhanced their durability and reliability.

Thickness-Dependent Healing of AgNW/$(PCL/PVA)_n$ Films. The thickness of the $(PCL/PVA)_n$ film has a significant influence on the restoration of conductivity of the AgNW layer. As shown in Figure 6a, R_s of the AgNW/$(PCL/PVA)_n$ films after a cycle of the cutting/healing process decreased along with the increase in the number of deposition cycles of the $(PCL/PVA)_n$ films. SEM images in Figure 6b,c show gaps in the AgNW layers of the healed AgNW/$(PCL/PVA)_4$ and AgNW/$(PCL/PVA)_5$ films, respectively. The gap is electrically insulating, which results in reduced conductivity in the healed region. The reduced number of gaps in the AgNW/$(PCL/PVA)_5$ film compared with that in the AgNW/$(PCL/PVA)_4$ film proves that a thicker PCL/PVA film allows for better restoration of conductivity after damage. To better demonstrate the thickness-dependent healing properties of the AgNW/$(PCL/PVA)_n$ films, morphologies of the healed $(PCL/PVA)_n$ films (with n being 4, 5, or 6) were measured by atomic force microscopy (AFM). These films were cut with a scalpel and healed by heating on a hot plate. As shown in the AFM images in Figure 6d–f, incomplete filling of the surrounding PCL and PVA to the damaged area resulted in the concave surface in the healed region of the $(PCL/PVA)_n$ films. Given that the AgNW layer moves along with the PCL/PVA layer during the healing process, the AgNW layer was thus stretched longer in the healed region because of the concave surface, which inevitably leads to formation of a gap in the AgNW layer. The concavities of the healed $(PCL/PVA)_n$ films increase along with the decline in number of film deposition cycles (scan lines in Figure 6d–f). As a result, the AgNW layer deposited on a thinner PCL/PVA film was stretched longer, leading to more gaps and enhanced R_s. Hence, thick PCL/PVA films are preferred to better restore conductivity in AgNW/$(PCL/PVA)_n$ films.

CONCLUSIONS

In summary, we have fabricated an NIR light-enabled healable, highly flexible and conductive film by depositing an AgNW layer on top of PCL/PVA composite film. Under low-power NIR light irradiation, the AgNW/$(PCL/PVA)_6$ film can quickly and finely restore conductivity loss caused by damage such as cuts and cracks that are several tens of micrometer wide. The AgNW layer functions not only as an electrical conductor but also as a NIR light-induced heater to initiate the healing of PCL/PVA film, which then imparts its healability to the conductive AgNW layer. Owing to the intrinsic healing nature of the PCL/PAA composite film, the AgNW/$(PCL/PVA)_6$ film can be cut and healed in the same region multiple times without apparent loss of its original conductivity. This work is the first to utilize low-power NIR light to repair electrically conductive films. When the advantages of NIR light are considered, such as easy availability, capacity for remote control, and precise location, NIR light allows for the healing process to be conveniently performed in ambient conditions without adversely affecting the surrounding components. Given the high conductivity, flexibility, and simple healable property of the conductive films, these films are believed to have practical applications in various optoelectronic devices with enhanced durability and reliability.

ASSOCIATED CONTENT

Supporting Information

Three figures showing dependence of spin-coated PCL film thickness on number of deposition cycles; UV–vis absorption spectra of $(PCL/PVA)_6$, AgNW, and AgNW/$(PCL/PVA)_6$; and self-healing ability test of AgNW/$(PS/PVA)_6$ film; and a movie of real-time healing of AgNW/$(PCL/PVA)_6$ film connected in a circuit with a commercially available light-emitting diode bulb. This material is available free of charge via the Internet at http://pubs.acs.org.

AUTHOR INFORMATION

Corresponding Author

*E-mail sun_junqi@jlu.edu.cn.

Author Contributions

The manuscript was written through contributions of all authors. All authors have given approval to the final version of the manuscript.

Funding

This work was supported by the National Natural Science Foundation of China (NSFC Grants 21225419 and 21221063) and the National Basic Research Program (2013CB834503).

Notes

The authors declare no competing financial interest.

■ ABBREVIATIONS

AgNW, silver nanowire; PCL, polycaprolactone; PVA, poly(vinyl alcohol); NIR, near-infrared

■ REFERENCES

(1) Williams, K. A.; Boydston, A. J.; Bielawski, C. W. Towards Electrically Conductive, Self-Healing Materials. *J. R. Soc. Interface* **2007**, *4*, 359−362.
(2) Blaiszik, B. J.; Kramer, S. L. B.; Olugebefola, S. C.; Moore, J. S.; Sottos, N. R.; White, S. R. Self-Healing Polymers and Composites. *Annu. Rev. Mater. Res.* **2010**, *40*, 179−211.
(3) Hager, M. D.; Greil, P.; Leyens, C.; Zwaag, S.; van der Schubert, U. S. Self-Healing Materials. *Adv. Mater.* **2010**, *22*, 5424−5430.
(4) Bergman, S. D.; Wudl, F. Mendable Polymers. *J. Mater. Chem.* **2008**, *18*, 41−62.
(5) Shchukin, D. G.; Möhwald, H. Self-Repairing Coatings Containing Active Nanoreservoirs. *Small* **2007**, *3*, 926−943.
(6) Benight, S. J.; Wang, C.; Tok, J. B. H.; Bao, Z. Stretchable and Self-Healing Polymers and Devices for Electronic Skin. *Prog. Polym. Sci.* **2013**, *38*, 1961−1977.
(7) Wojtecki, R. J.; Meador, M. A.; Rowan, S. J. Using the Dynamic Bond to Access Macroscopically Responsive Structurally Dynamic Polymers. *Nat. Mater.* **2011**, *10*, 14−27.
(8) Chung, C.-M.; Roh, Y.-S.; Cho, S.-Y.; Kim, J.-G. Crack Healing in Polymeric Materials via Photochemical [2 + 2] Cycloaddition. *Chem. Mater.* **2004**, *16*, 3982−3984.
(9) Yang, Y.; Urban, M. W. Self-Healing Polymeric Material. *Chem. Soc. Rev.* **2013**, *42*, 7446−7467.
(10) White, S. R.; Sottos, N. R.; Geubelle, P. H.; Moore, J. S.; Kessler, M. R.; Sriram, S. R.; Brown, E. N.; Viswanathan, S. Autonomic Healing of Polymer Composites. *Nature* **2001**, *409*, 794−797.
(11) Wilson, G. O.; Caruso, M. M.; Reimer, N. T.; White, S. R.; Sottos, N. R.; Moore, J. S. Evaluation of Ruthenium Catalysts for Ring-Opening Metathesis Polymerization-Based Self-Healing Applications. *Chem. Mater.* **2008**, *20*, 3288−3297.
(12) Park, J.-H.; Braun, P. V. Coaxial Electrospinning of Self-Healing Coatings. *Adv. Mater.* **2010**, *22*, 496−499.
(13) Zheludkevich, M. L.; Shchukin, D. G.; Yasakau, K. A.; Möhwald, H.; Ferreira, M. G. S. Anticorrosion Coatings with Self-Healing Effect Based on Nanocontainers Impregnated with Corrosion Inhibitor. *Chem. Mater.* **2007**, *19*, 402−411.
(14) Li, G. L.; Zheng, Z.; Möhwald, H.; Shchukin, D. G. Silica/Polymer Double-Walled Hybrid Nanotubes: Synthesis and Application as Stimuli-Responsive Nanocontainers in Self-Healing Coatings. *ACS Nano* **2013**, *7*, 2470−2478.
(15) Li, Y.; Li, L.; Sun, J. Bioinspired Self-Healing Superhydrophobic Coatings. *Angew. Chem., Int. Ed.* **2010**, *49*, 6129−6133.
(16) Cordier, P.; Tournilhac, F.; Soulié-Ziakovic, C.; Leibler, L. Self-Healing and Thermoreversible Rubber from Supramolecular Assembly. *Nature* **2008**, *451*, 977−980.
(17) Iyer, A. St. J.; Lyon, L. A. Self-Healing Colloidal Crystals. *Angew. Chem., Int. Ed.* **2009**, *48*, 4562−4566.
(18) Wang, X.; Liu, F.; Zheng, X.; Sun, J. Water-Enabled Self-Healing of Polyelectrolyte Multilayer Coatings. *Angew. Chem., Int. Ed.* **2011**, *50*, 11378−11381.
(19) Wang, X.; Wang, Y.; Bi, S.; Wang, Y.; Chen, X.; Qiu, L.; Sun, J. Optically Transparent Antibacterial Films Capable of Healing Multiple Scratches. *Adv. Funct. Mater.* **2014**, *24*, 403−411.
(20) Chen, Y.; Kushner, A. M.; Williams, G. A.; Guan, Z. Multiphase Design of Autonomic Self-Healing Thermoplastic Elastomers. *Nat. Chem.* **2012**, *4*, 467−472.
(21) Lei, Z. Q.; Xiang, H. P.; Yuan, Y. J.; Rong, M. Z.; Zhang, M. Q. Room-Temperature Self-Healable and Remoldable Cross-linked Polymer Based on the Dynamic Exchange of Disulfide Bonds. *Chem. Mater.* **2014**, *26*, 2038−2046.
(22) Zheng, P.; McCarthy, T. J. A Surprise from 1954: Siloxane Equilibration Is a Simple, Robust, and Obvious Polymer Self-Healing Mechanism. *J. Am. Chem. Soc.* **2012**, *134*, 2024−2027.
(23) Zhang, H.; Xia, H.; Zhao, Y. Poly(vinyl alcohol) Hydrogel Can Autonomously Self-Heal. *ACS Macro Lett.* **2012**, *1*, 1233−1236.
(24) Ghosh, B.; Urban, M. W. Self-Repairing Oxetane-Substituted Chitosan Polyurethane Networks. *Science* **2009**, *323*, 1458−1460.
(25) Cong, H.-P.; Wang, P.; Yu, S.-H. Stretchable and Self-Healing Graphene Oxide−Polymer Composite Hydrogels: A Dual-Network Design. *Chem. Mater.* **2013**, *25*, 3357−3362.
(26) Zhang, M.; Xu, D.; Yan, X.; Chen, J.; Dong, S.; Zheng, B.; Huang, F. Self-Healing Supramolecular Gels Formed by Crown Ether Based Host−Guest Interactions. *Angew. Chem., Int. Ed.* **2012**, *51*, 7011−7015.
(27) Yan, X.; Xu, D.; Chen, J.; Zhang, M.; Hu, B.; Yu, Y.; Huang, F. A Self-Healing Supramolecular Polymer Gel with Stimuli-Responsiveness Constructed by Crown Ether Based Molecular Recognition. *Polym. Chem.* **2013**, *4*, 3312−3322.
(28) Burnworth, M.; Tang, L.; Kumpfer, J. R.; Duncan, A. J.; Beyer, F. L.; Fiore, G. L.; Rowan, S. J.; Weder, C. Optically Healable Supramolecular Polymers. *Nature* **2011**, *472*, 334−337.
(29) Hentschel, J.; Kushner, A. M.; Ziller, J.; Guan, Z. Self-Healing Supramolecular Block Copolymers. *Angew. Chem., Int. Ed.* **2012**, *51*, 10561−10565.
(30) Caruso, M. M.; Schelkopf, S. R.; Jackson, A. C.; Landry, A. M.; Braun, P. V.; Moore, J. S. Microcapsules Containing Suspensions of Carbon Nanotubes. *Mater. Chem.* **2009**, *19*, 6093−6096.
(31) Odom, S. A.; Caruso, M. M.; Finke, A. D.; Prokup, A. M.; Ritchey, J. A.; Leonard, J. H.; White, S. R.; Sottos, N. R.; Moore, J. S. Restoration of Conductivity with TTF-TCNQ Charge-Transfer Salts. *Adv. Funct. Mater.* **2010**, *20*, 1721−1727.
(32) Blaiszik, B. J.; Kramer, S. L. B.; Grady, M. E.; McIlroy, D. A.; Moore, J. S.; Sottos, N. R.; White, S. R. Autonomic Restoration of Electrical Conductivity. *Adv. Mater.* **2012**, *24*, 398−401.
(33) Li, Y.; Chen, S.; Wu, M.; Sun, J. Polyelectrolyte Multilayers Impart Healability to Highly Electrically Conductive Films. *Adv. Mater.* **2012**, *24*, 4578−4582.
(34) Tee, B. C-K.; Wang, C.; Allen, R.; Bao, Z. An Electrically and Mechanically Self-Healing Composite with Pressure- and Flexion-Sensitive Properties for Electronic Skin Applications. *Nat. Nanotechnol.* **2012**, *7*, 825−832.
(35) Palleau, E.; Reece, S.; Desai, S. C.; Smith, M. E.; Dickey, M. D. Self-Healing Stretchable Wires for Reconfigurable Circuit Wiring and 3D Microfluidics. *Adv. Mater.* **2013**, *25*, 1589−1592.
(36) Wang, H.; Zhu, B.; Jiang, W.; Yang, Y.; Leow, W. R.; Wang, H.; Chen, X. Mechanically and Electrically Self-Healing Supercapacitor. *Adv. Mater.* **2014**, *26*, 3638−3643.
(37) Gong, C.; Liang, J.; Hu, W.; Niu, X.; Ma, S.; Hahn, H. T.; Pei, Q. Healable, Semitransparent Silver Nanowire-Polymer Composite Conductor. *Adv. Mater.* **2013**, *25*, 4186−4191.
(38) Tao, A.; Kim, F.; Hess, C.; Goldberger, J.; He, R.; Sun, Y.; Xia, Y.; Yang, P. Langmuir−Blodgett Silver Nanowire Monolayers for Molecular Sensing Using Surface-Enhanced Raman Spectroscopy. *Nano Lett.* **2003**, *3*, 1229−1233.
(39) Hu, L.; Kim, H. S.; Lee, J.-Y.; Peumans, P.; Cui, Y. Scalable Coating and Properties of Transparent, Flexible, Silver Nanowire Electrodes. *ACS Nano* **2010**, *4*, 2955−2963.
(40) Liang, J.; Li, L.; Tong, K.; Ren, Z.; Hu, W.; Niu, X.; Chen, Y.; Pei, Q. Silver Nanowire Percolation Network Soldered with Graphene

Oxide at Room Temperature and Its Application for Fully Stretchable Polymer Light-Emitting Diodes. *ACS Nano* **2014**, *8*, 1590−1600.
(41) Li, Y.; Cui, P.; Wang, L.; Lee, H.; Lee, K.; Lee, H. Highly Bendable, Conductive, and Transparent Film by an Enhanced Adhesion of Silver Nanowires. *ACS Appl. Mater. Interfaces* **2013**, *5*, 9155−9160.
(42) Chen, S.-P.; Kao, Z.-K.; Lin, J.-L.; Liao, Y.-C. Silver Conductive Features on Flexible Substrates from a Thermally Accelerated Chain Reaction at Low Sintering Temperatures. *ACS Appl. Mater. Interfaces* **2012**, *4*, 7064−7068.
(43) Garnett, E. C.; Cai, W.; Cha, J. J.; Mahmood, F.; Connor, S. T.; Christoforo, M. G.; Cui, Y.; McGehee, M. D.; Brongersma, M. L. Self-Limited Plasmonic Welding of Silver Nanowire Junctions. *Nat. Mater.* **2012**, *11*, 241−249.
(44) Huang, X.; Qian, Q.; Zhang, X.; Du, W.; Xu, H.; Wang, Y. Assembly of Carbon Nanotubes on Polymer Particles: Towards Rapid Shape Change by Near-Infrared Light. *Part. Part. Syst. Charact.* **2013**, *30*, 235−240.